

The geothermal reservoir of Hainaut: the result of thermal convection in a carbonate and sulfate aquifer

LUCIANE LICOUR

Université de Mons, Faculté Polytechnique, Geology and Applied Geology Department, Place du Parc, 20, 7000 Mons. E-mail: Luciane.licour@umons.ac.be

ABSTRACT. The geothermal reservoir of Hainaut mainly consists in a fissured and karstic carbonate aquifer. It is composed of thick Lower Carboniferous limestone and dolostone formations with an E-W direction and a 10-15° south dip. In the Saint-Ghislain area, several layers of massive anhydrite are interbedded in the Upper and Middle Visean carbonate. Coeval formations in other areas consist of a collapse breccia suggesting that the entire anhydrite/carbonate sequence has been subjected to karstification. The existence of a deep karst in the Visean of Hainaut is supported by several indications, as, for example, the occurrence of abundant karstic pipes observed in the whole Upper Carboniferous formations. The overlying Mons Basin is also thought to be (at least partly) the result of karstic subsidence in the Visean basement. Anomalies in temperature and/or chemical and isotopic signatures in springs and water catchment wells of the Dinantian outcrop suggest moderate uprising flow of geothermal deep groundwater and mixing with shallow groundwater. Flow and heat transfers have been simulated using simplified models. Results corroborate the existence of large thermal-induced convection loops within the Dinantian reservoir. Karst development in the deep Lower Carboniferous strata of Hainaut is related to an increase of permeability due to tectonic activity that initiated at least at the end of Jurassic, that allowed the initiation of thermal convection. This time estimation is consolidated by sedimentologic data on Cretaceous deposits in the Mons Basin.

KEYWORDS : Geothermal energy, Mons Basin, convective flow, karst

RESUME. Le réservoir géothermique du Hainaut : Le résultat de la convection thermique dans un aquifère carbonaté et sulfaté. Le réservoir géothermique du Hainaut est un aquifère fissuré karstique, composé de calcaires et dolomies du Carbonifère inférieur, de direction E-W, et affectés d'un pendage moyen de 10 à 15° sud. Dans la région de Saint-Ghislain, des niveaux d'anhydrite massive sont présents dans les calcaires du Viséen moyen et supérieur. Les formations équivalentes latéralement sont des brèches d'effondrement, suggérant que l'ensemble de la série d'anhydrites et les carbonates interstratifiés ont été sujets à la karstification. L'hypothèse de l'existence d'un karst profond dans le Viséen du Hainaut est supportée par plusieurs indices, par exemple la présence de nombreux puits d'effondrement karstiques à travers les terrains du Carbonifère supérieur. Le Bassin de Mons sus-jacent est également tenu (partiellement du moins) pour une conséquence de la subsidence karstique due aux dissolutions dans le Viséen. Des anomalies thermiques, chimiques et isotopiques dans les sources et puits de pompage de l'aquifère dinantien sub-affleurant confirment la remontée d'eaux géothermiques profondes et leur mélange avec les eaux peu profondes. Les écoulements et transferts de chaleur ont été simulés dans un modèle simplifié. Les résultats confirment l'existence de larges boucles de convection dans le réservoir dinantien. Le développement du karst dans le Dinantien profond du Hainaut est relié à l'augmentation de perméabilité elle-même due à l'activité tectonique extensive mise en place au moins à partir du Jurassique terminal. Cette estimation temporelle est étayée par des arguments sédimentologiques présents dans les dépôts crétacés du Bassin de Mons.

MOTS CLES: Energie géothermique, Bassin Mons, convection thermique, karst

1. Introduction

The geothermal exploitation site of Hainaut is located in the Mons region (Fig. 1). Three wells were drilled between Mons and the French border, in Saint-Ghislain, Douvrain and Ghlin (Delmer, 1977; Leclercq, 1980; Delmer et al., 1982; Delmer et al., 1996). Each of them can produce hot water (approximately 70°C), at an artesian natural flow rate of 100 m³/h. The productive layers are located at 2500 m, 1375 m and 1575 m deep, respectively. The first two wells are currently in use for district heating applications. The third one will soon be connected to its own heating network.

Several new projects are currently in progress in the Hainaut region, including the drilling of a new well near Mons. In the meantime, recent research has been led regarding the geological structure of the geothermal reservoir and its hydraulic characteristics (Licour et al., 2007; Licour, 2009; Licour et al., 2011; Licour, 2012). This paper presents some of these results, which give new insights regarding the explanation of karstification in deep aquifers of Hainaut and offer new perspectives for geothermal exploitation, notably in terms of spatial extension. These results are described in the next sections.

2. Geological setting

2.1. Paleozoic bedrock of the Mons Basin

The geothermal reservoir is located in the Lower Carboniferous (Mississippian, previously Dinantian) and Upper Devonian aquifer that lies under the coal measures and the Meso-Cenozoic Mons Basin (Figs 2 and 3). The Dinantian aquifer outcrops a few kilometers north of the existing geothermal wells. It mainly consists in carbonates (limestone and dolostone) (Bultynck & Dejonghe, 2001; Poty et al., 2001; Delmer et al., 2001), but also contains more detritic formations close to the bottom and top of Dinantian. These detritic strata include phanerites of the Dinantian-Namurian transition and shales and sandstones of Lower Tournaisian, Famennian and Upper Frasnian (see Fig. 3). Evaporites were also observed in the Saint-Ghislain borehole (see Fig. 4), in the Upper and Middle Visean series (Dejonghe et al., 1976; Rouchy et al., 1984; De Putter et al., 1991). More detail is given about these deposits in Section 3.

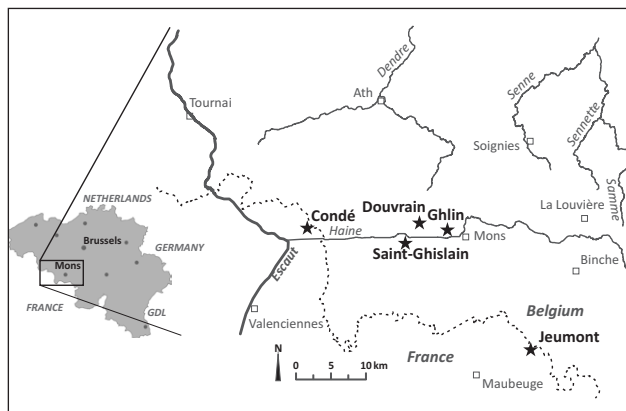


Figure 1. Localization of the geothermal exploitation area of Hainaut. The 3 geothermal wells are symbolized by a star. The Jeumont borehole and the Condé-sur-Escaut well are also represented.

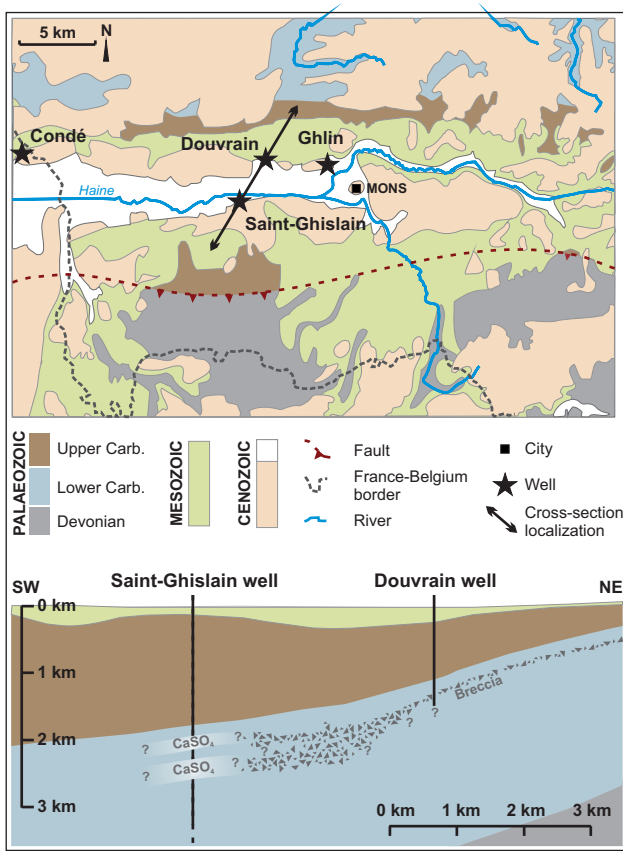


Figure 2. Simplified geological map (above) and vertical cross section (below) of the Mons Basin.

2.2. Structural setting

Variscan tectonic has induced several structural units in the Paleozoic bedrock of Belgium and surrounding countries (Mansy et al., 1999; Vanbrabant et al., 2002; Mansy & Lacquement, 2006; Bélanger et al., 2012). The geothermal reservoir is part of the Brabant Parautochton unit that lies under the Ardennes Allochthon and the Overturned Thrust-Sheets (OTS) of Haine-Sambre-Meuse, a complex of several thrust-sheets determined by the series of thrust faults that constitutes the Variscan Front. The Dinantian reservoir shows few folds and faults, in comparison with the tectonical complexity of the overlying units (Lacquement et al., 1999; Delmer, 2004; Vandycke, 2007).

Older tectonic can be observed when comparing the thicknesses of formations between the Saint-Ghislain (Groessens et al., 1979) and the Jeumont boreholes (Delmer, 1988), located 20 km southeastward (Fig 1). The important thickening of the Devonian and Carboniferous deposits in the Saint-Ghislain

region suggests synsedimentary movements due to ante-Variscan subsidence (Meilliez, 1989; Ziegler, 1990; Mansy & Meilliez, 1993; Mansy & Lacquement, 2006). This context may imply discontinuities in the Dinantian reservoir and must be taken into account for resource characterization and estimation.

2.3. Regional subsidence and Post-Paleozoic sediments

The Mons Basin contains Meso-Cenozoic sediments trapped in a subsident structure (Delmer, 1972; De Magnée et al., 1986; Rouchy et al., 1986). The top of the Paleozoic bedrock is relatively well known thanks to coal mining industry. Isohypses maps of this surface have been produced (Stevens & Marlière, 1944; Cordonnier, 1984) and show a basin-like irregular structure oriented E-W (see section 3.2.3). Detailed studies about Cretaceous sediments (Dupuis & Vandycke, 1989; Spagna, 2010) demonstrate the displacement of the subsidence maxima toward the South during Cretaceous times. Wealden facies deposits position on the north flank of the structure (Spagna, 2010) fossilizes the early Mons Basin before its later progression.

3. Karstic features in the Dinantian of Hainaut and impact on overlying strata

3.1. Karst in shallow formations

Superficial karst features have been investigated for years in the Carboniferous limestones of Hainaut (Quinif, 1989; Quinif et al.,

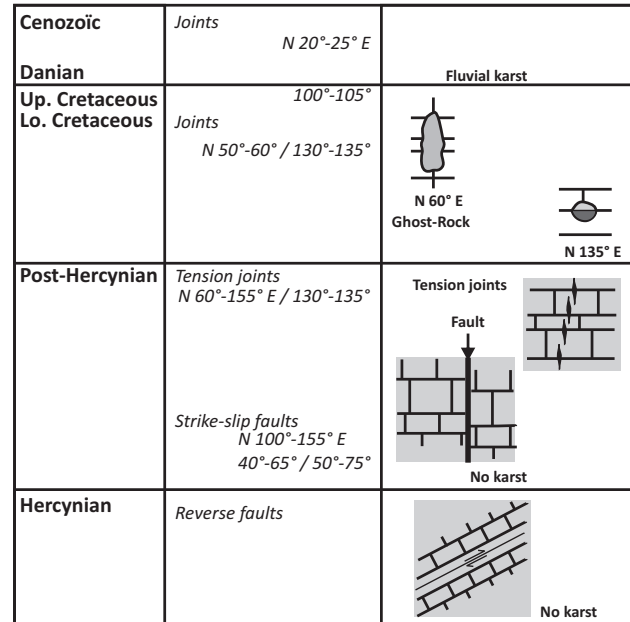


Figure 4. Relations between karst and tectonic in the Carboniferous Limestone of the Hainaut region (from Vergari & Quinif, 1997).

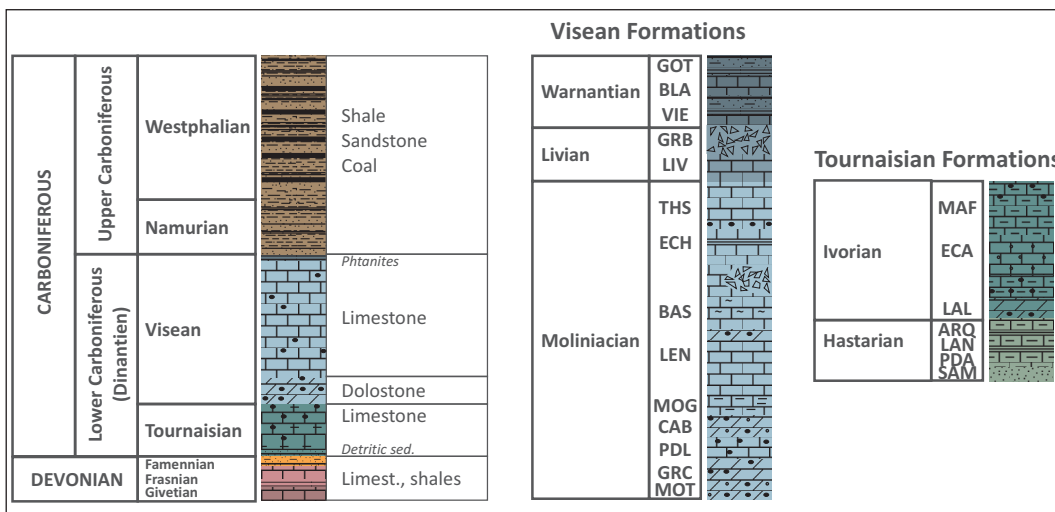


Figure 3. Synthetic lithostratigraphic log of the Devon-Carboniferous outcrops of the Brabant Parautochton in Hainaut. The two additional logs give more detail on Visean and Tournaisian formations. Breccia layers can be found in Upper and Middle Dinantian, in the Basècles and Grande Brèche Formations (BAS et GRB).

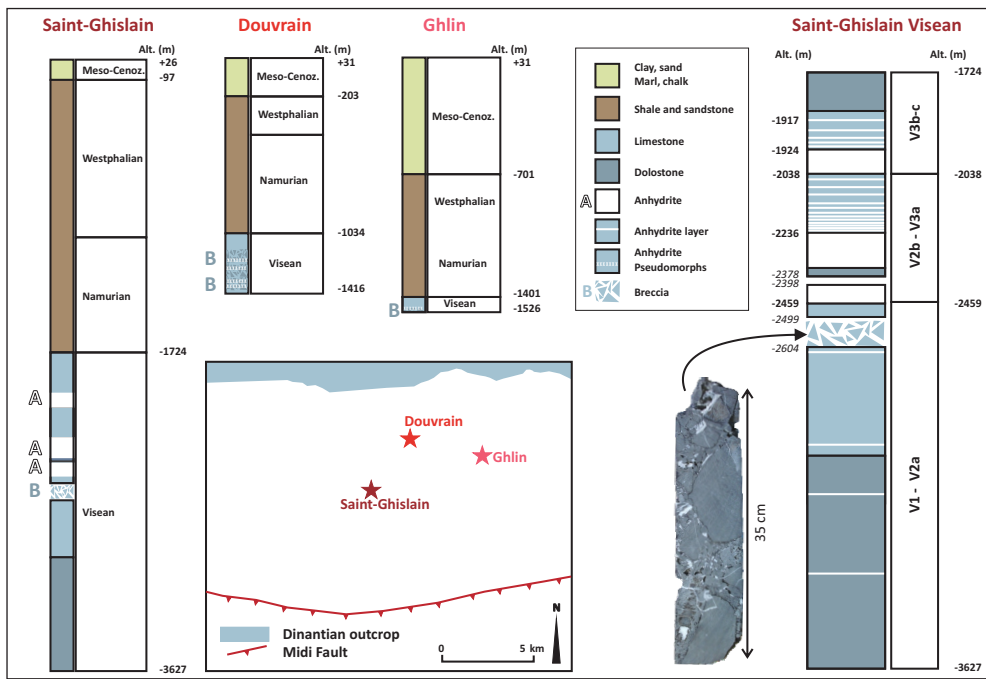


Figure 5. Visean strata in the geothermal wells of Hainaut. Anhydrite and breccia layers are represented on the simplified logs. Visean formations in the Saint-Ghislain borehole are given with more detail on the right log. The wells location is given on the map (Licour, 2012).

1993; Vergari & Quinif, 1997; Quinif et al., 1997; Kaufmann, 2000; Quinif et al., 2006; Havron et al., 2007), mainly in the Soignies and Tournai regions where quarries activity implies increasing concern about water pumping and stability related to karst. Previous studies (Vergari & Quinif, 1997; Quinif et al., 1997) have determined the strong relation between karstic occurrences and regional extensive tectonic context (Fig. 4), resulting in preferential karstified directions.

Paleogeographical conditions, and more specifically the relief evolution and the eustatic variations, influence the formation of the different karstic features depending on hydraulic regime, among which the “ghost rock” karst corresponding to low hydraulic potential (Vergari and Quinif, 1997).

3.2. Karst in deep formations

3.2.1 Breccias

The deep karst of the Dinantian aquifer seems strongly linked to the presence of Visean evaporites and their partial dissolution. Massive anhydrite still exists in Saint-Ghislain (Groessens et al., 1979; Rouchy et al., 1984; De Putter et al., 1994), and has been replaced laterally by collapse breccias (Leclercq, 1980; Delmer et al., 1982; Rouchy et al., 1984; Mamet et al., 1986; De Magnée et al., 1986; Rouchy et al., 1986; De Putter, 1995) that can be seen in the two other geothermal wells (Fig. 5) and in outcropping rocks of the Basècles and the Grande Brèche formations, respectively noted BAS and GRB on Fig. 3.

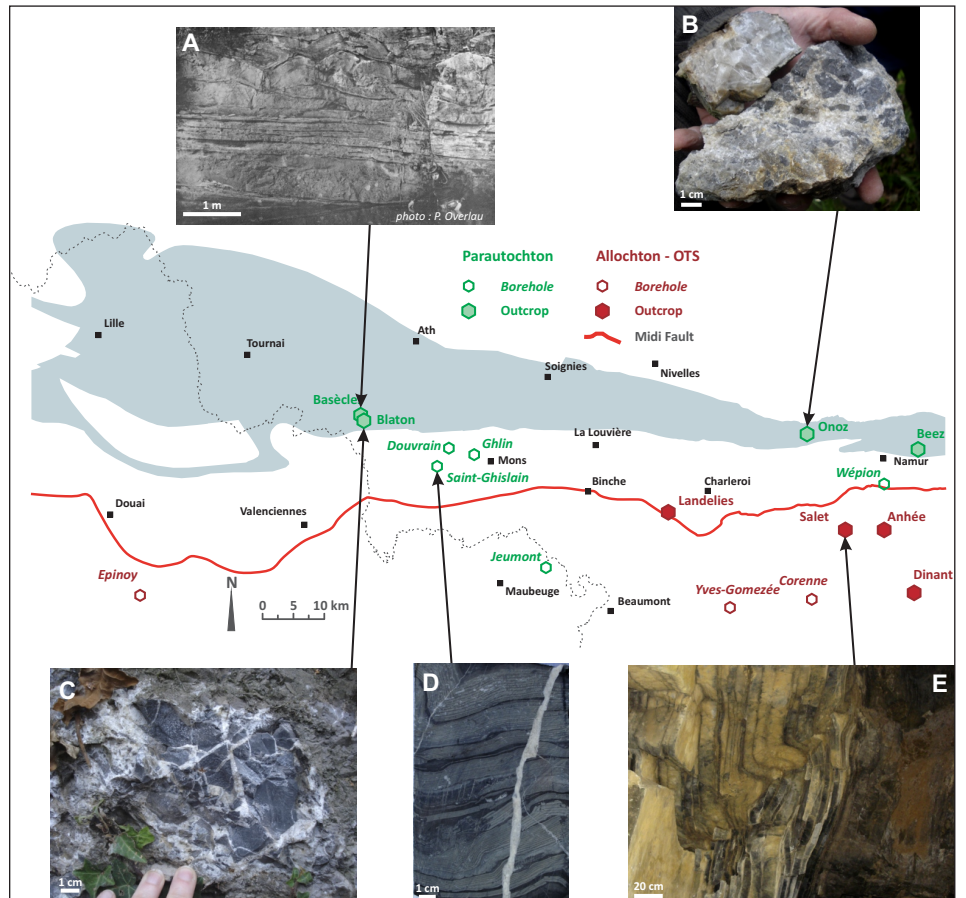


Figure 6. Visean breccias observed at the outcrop or in borehole. The map represents several breccia occurrences in different structural units. Some of them are illustrated by pictures to highlight the differences in aspect. A : Slumpings in the Middle Visean in Basècles quarries (Overlaau, 1966). B : Breccia from the Grande Brèche Formation in Onoz. C : Breccia from the Grande Brèche Formation in Blaton. D : Slumping features in Upper Visean cores of the Saint-Ghislain borehole. E : Slumping features in the Middle Devonian of Salet.

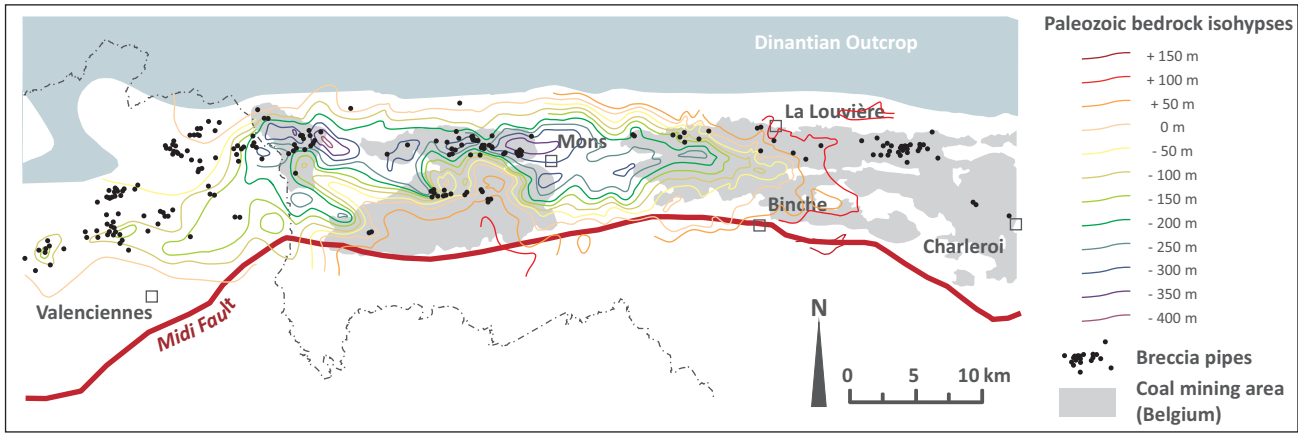


Figure 7. Top of the Paleozoic bedrock of the Mons Basin, isohyps map (from Stevens & Marlière, 1944) and breccia pipes in the Hainaut region (from Delmer & Van Wichelen, 1980). The grey areas show the extension of coal mining operations.

3.2.2 Breccias formation model

Different types of breccias co-exist in Dinantian series, and show different facies. Fig. 6 localizes some of these breccia occurrences, in both parautochton and allochton units. They can be the result of many phenomena (Overlau, 1963; Overlau, 1966; Fiege et al., 1967; Hance & Hennebert, 1980; Hance et al., 1981; Mamet et al., 1986; De Magnée et al., 1986; Rouchy et al., 1986; Rouchy et al., 1993; De Putter, 1995), among which slumping, erosion/deposition, tectonic influence and karstic collapse.

The Hainaut Visean breccias seem to be related to two possible origins at two different periods: slumping (synsedimentary) and karstic collapse due to evaporites dissolution occurring during the Meso-Cenozoic extensional phase.

3.2.3 Other indications of karst activity

Consequences of karstic activity during the Cretaceous and Paleogene can be found through the existence of numerous karstic pipes across the Upper Carboniferous strata and in the regional subsidence that has affected the Mons region at that period, causing the Cretaceous and Cenozoic deposits conservation.

The breccia pipes are roughly cylindrical structures observed across the Upper Carboniferous strata. Their dimensions range from a few meters to several hundreds of meters laterally, and can reach several hundreds of meters vertically. Their extension limit (Fig. 7) corresponds to the subsided region evoked at section 2.3, illustrated on Fig. 7 by the isohyps of the Paleozoic surface (Delmer & Van Wichelen, 1980; Spagna, 2010; Quinif & Licour, 2012; Licour, 2012). They mostly contain brecciated coal measures, but also sometimes caused the trapping of sediments from the contemporary surface. Therefore, they allow an estimation of the active karstic period corresponding to their formation (Delmer & Van Wichelen, 1980). The Ghlin well, drilled into a karstic pipe, demonstrates the origin of the

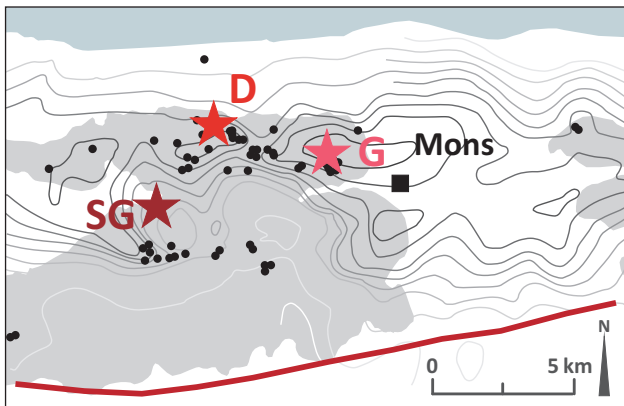


Figure 8. The geothermal wells area (zoom of Fig. 7, see Fig. 7 for the legend), breccia pipes, coal mined areas and isohyps of the Paleozoic. SG, D and G refer to the three geothermal wells of Saint-Ghislain, Douvrain and Ghlin respectively.

dissolution in the deep Dinantian (Delmer et al., 1982), as it touched both the brecciated Upper Visean and permeable breccias laterally correlated to the Grande Brèche formation (Figs 3 and 5).

3.3 Deep dissolution model

The Saint-Ghislain region (Fig. 8) shows some particularities that can lead to several hypotheses about the dissolution processes in the deep Lower Carboniferous strata. First, the coincidence between the subsidence of the Paleozoic bedrock and the breccia pipes spatial distribution is obvious. Second, the breccia pipes are absent around the Saint-Ghislain region. The intensive coal mining activity in this area would have highlighted them if present (Licour, 2009).

A schematic model can be drawn from these observations (Friedman, 1997; Licour, 2012), based among others on the difference in mechanical behavior between anhydrite and limestone (Fig. 9). Where the limestone shows fragile rupture if a cavity forms within its strata, anhydrite shows ductile deformation and prevents the formation of sinkholes. Supposing a fresh water influx through joints and fractures, the formation of breccia pipes is observed at a local scale. Then, lateral spreading leading to regional subsidence can be suggested.

This model supposes the removal of large quantities of anhydrite, and then implies the existence of continuous groundwater flow for solution replacement and dissolution products elimination. Hydraulic gradient is of course at the origin of flow in the sub-superficial part of the aquifer. However, an additional source of power is needed to explain deep groundwater circulation.

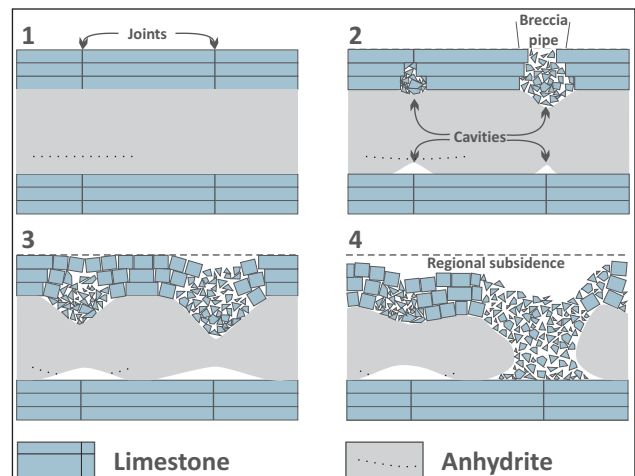


Figure 9. Schematic model of dissolution of a thick saline stratum (Licour, 2012, from Friedman, 1997, modified). Dissolution starts at fractures and joints (1), causing the rupture of overlying strata, then propagates laterally. The breccias pipes occur first (2), and can be followed by regional subsidence (3 and 4).

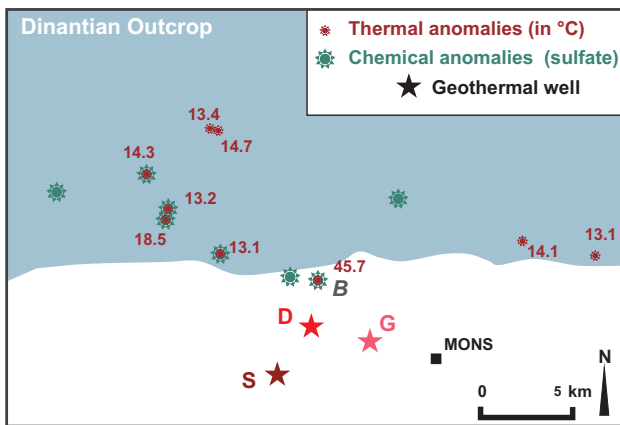
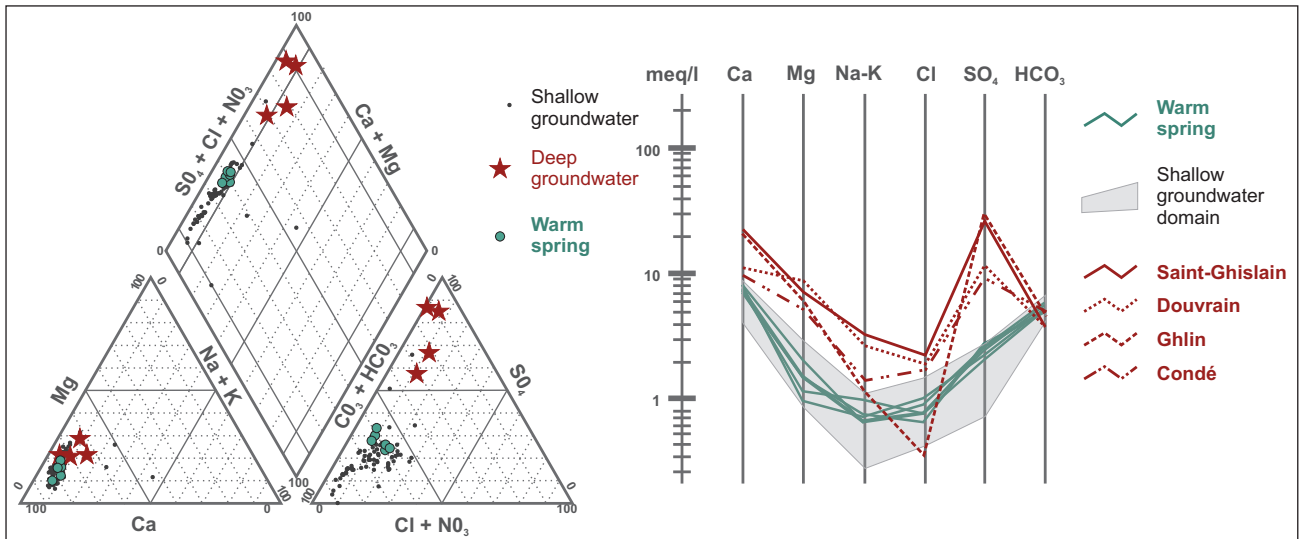


Figure 10. a. Localization of warm and/or sulfated springs at the Dinantian outcrop. b. Chemical content of shallow groundwater, deep groundwater and warm spring water on the Piper and Schoeller-Berkaloff diagrams.



4. Flow in the Dinantian reservoir

4.1. Thermal and chemical traces of deep water exurgence

Water upflow from the deep reservoir toward the surface is suggested by thermal and chemical arguments: several springs and groundwater pumping in the shallow part of the Dinantian aquifer show warm temperatures and high sulfate content (Fig. 10a) (Bosch et al., 1981; Delmer et al., 1982; Blommaert et al., 1983; Licour, 2012). Sulfate resulting from anhydrite dissolution can be considered as the chemical signature of deep waters (see Fig. 10b). Nevertheless, evaporites dissolution may not be the only

possible origin for dissolved sulfate in water. The Carboniferous limestone actually contains pyrite and other sulfides that can also give sulfates if oxidized.

In this context, isotopic geochemistry is helpful for sulfate origin determination (Holser & Kaplan, 1966; Krouse, 1980; Pearson & Rightmire, 1980; Mook, 2000). Evaporitic sulfate shows positive isotopic ratios for $\delta^{18}\text{O}$ and $\delta^{34}\text{S}$ in sulfate ion, and sulfate resulting from sulfide oxidation shows negative isotopic ratios. Deep groundwater samples are located in the evaporitic domain of the $\delta^{34}\text{S}/\delta^{18}\text{O}$ diagram (Fig. 11). Only one of the shallow groundwaters, sampled in a spring originating from a pyrite-rich alterite, represents the sulfide domain of the diagram.

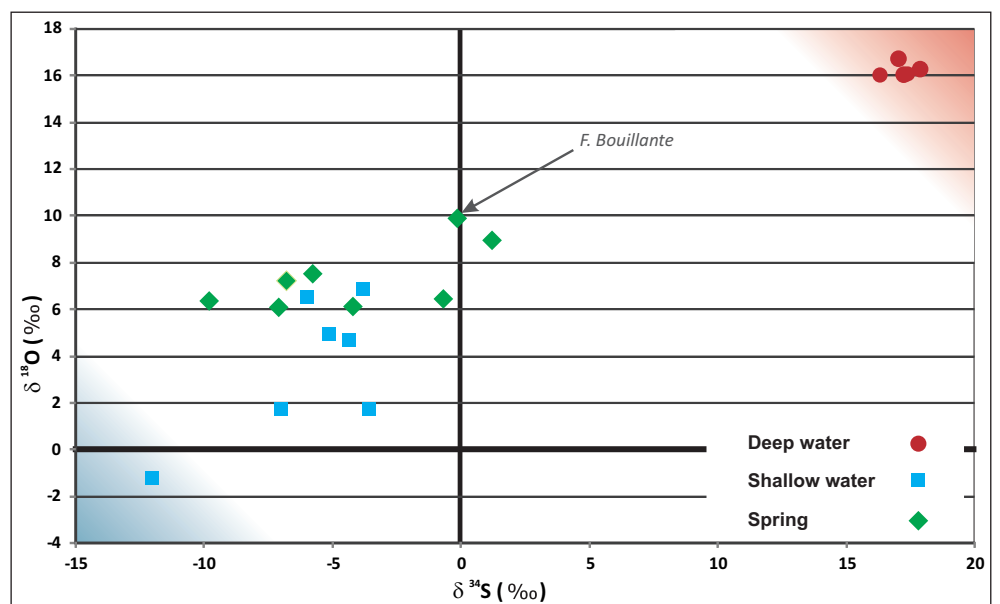


Figure 11. $\delta^{34}\text{S}$ and $\delta^{18}\text{O}$ in dissolved sulfate in shallow water, deep water and warm springs of the Dinantian reservoir. Deep water appears in the positive ratios area, showing their evaporitic origin. The opposite corner of the diagram refers to negative ratios indicating sulfates resulting on sulfide oxidation. The arrow points to symbols representing warm springs with a higher evaporitic sulfate content, among which the “Fontaine Bouillante”.

The other samples, including most of the warm and sulfated springs, take place between these two categories of groundwaters. Their sulfate content can thus be considered as of mixed origin. Several spring waters are closer to the evaporitic domain. One of these springs is the famous “Fontaine Bouillante”, which shows a 18°C constant temperature throughout the year. Their location on the diagram confirms the more important contribution of deep water in their sulfate content.

A possible assumption is that the outcropping part of the Dinantian aquifer could be considered as both the recharge and the discharge area of the deep geothermal reservoir. Meteoric water that infiltrates the deep aquifer flows back to the surface by convection forces, after heating and changing in geochemical and isotopic signature by contact with the rock matrix or mixing with hot sulfated water (Licour, 2012).

4.2. Convective flow

The existence of thermal convection in a porous medium is conditioned by the following equation (Combarous & Bories, 1975): $\text{Ra} \cdot \cos \gamma \geq 4 \pi^2$

Ra is the Rayleigh number dependant on the fluid characteristics, the permeability of the porous medium, its thickness and the temperature gradient. γ is the dip of the porous stratum.

In the Saint-Ghislain region, the condition is met for thermal convection to occur in the deep reservoir. This is consistent with the observed temperatures of the geothermal fluid exploited in Douvrain and Ghlin, higher than expected considering the local geothermal gradient, and with the perturbations in the thermal profile of the Saint-Ghislain well (Legrand, 1978).

Flow and heat transfer have been simulated using SHEMAT (Clauser et al., 2013), a finite differences code adapted to hydrothermal reservoirs. A simplified model of a 13° dipping, 2000 m thick permeable layer ($k = 10^{-13} \text{ m}^2$) bounded by impervious top and bottom formations ($k = 10^{-20} \text{ m}^2$) has been realized (Fig. 12). The resulting simulated temperature and groundwater fluxes fields are consistent with measured temperatures and estimations of residence times in the reservoir based on residual ^{14}C activity (Licour, 2012). More information about these simulations can be found in Licour (2012).

In the aim of understanding the first steps of the deep reservoir formation and estimating the initial permeability that would be needed to start the convective flow, simulation has been tested with a regular thermal gradient of 2,5 °C/100 m, in a permeable 300 m thick unconfined stratum, without any hydraulic gradient. Thermal convection appears as soon as the Combarous & Bories (1975) condition is met, in this case with $k = 10^{-11} \text{ m}^2$, which is an average permeability in the present shallow reservoir. Thermal convection is then likely to be at the origin of regional flow circulation and anhydrite removal in the deep Dinantian reservoir. These phenomena caused the formation of collapse breccia layers and karstic pipes, and participated to regional subsidence in the Mons Basin area.

5. Conclusions

The existence of shallow karst in the Dinantian aquifer of Hainaut relates to the extensional tectonic regime occurring at least during the deposition of the Meso-Cenozoic sediments of the Mons Basin. Different karstic features co-exist, depending on paleogeographical conditions and hydraulic potential.

The propagation of karstification to the deep part of the aquifer, mainly in evaporitic thick strata, can be linked to the same phenomenon. The increase of permeability induced by fracturation in the carbonate formations leads to the initiation of thermal convection, even if the hydraulic potential is very low. Once initiated, convective flow brings more aggressive water toward soluble rocks and removes the dissolution products.

The dissolution of Visean evaporites and its propagation toward South had several effects on overlying strata. First, fresh water influxes through joints and fractures cause the formation of sinkholes and breccias pipes. Second, the lateral spreading of the dissolution participates to replace the thick strata of anhydrites by collapse breccia layers. These layers are met in two geothermal wells and at the Visean outcrop. Finally, the loss of volume in deep layers could have induced, among other possible causes, the regional subsidence and the trapping of Meso-Cenozoic sediments in the resulting Mons Basin.

The convective circulation is still active currently. The exurgence of deep water is attested by temperature anomalies and chemical and isotopic content of several springs and groundwater catchment wells in the shallow part of the Dinantian aquifer.

6. Acknowledgements

The author would like to thank the reviewers Vincent Hallet and Pascal Goderniaux for the valuable corrections and suggestions that greatly helped to make this manuscript both clearer and more complete.

7. References

- Bélanger, I., Delaby, S., Delambre, B., Ghysel, P., Hennebert, M., Laloux, M., Marion, J.-M., Mottequin, B. & Pingot, J.-L., 2012. Redéfinition des unités structurales du front varisque utilisées dans le cadre de la nouvelle Carte géologique de Wallonie (Belgique). *Geologica Belgica*, 15, 3, 169-175.
- Blommaert, W., Vandelannoote, R., Sadurski, A., Van't Dack, L. & Gijbels, R., 1983. Trace-elements geochemistry of thermal water percolating through a karstic environment in the region of Saint-Ghislain (Belgium). *Journal of Volcanology and Geothermal Research*, 19, 331–348.
- Bosch, B., Caulier, P., Leplat, J. & Talbot, A., 1981. Un objectif géothermique : Le Calcaire Carbonifère sous le Bassin Houiller à l'Est de Saint-Amand-les-Eaux. *Annales de la Société Géologique du Nord*, 100, 167–174.
- Bultynck, P. & Dejonghe, L., 2001. Devonian lithostratigraphic units (Belgium). *Geologica Belgica*, 4, 36–69.
- Clauser, C., Bartels, J., Cheng, L.-Z., Chiang, W.-H., Hurtere, S., Kühn, M., Meyn, V., Pape, H., Pribnow, D. F. C., Ranalli, G., Schneider, W. & Stöfen, H., 2003. Numerical simulation of reactive flow in hot aquifers – SHEMAT and Processing SHEMAT. Springer, 332 p.
- Combarous, M. A. & Bories, S. A., 1975. Hydrothermal convection in saturated porous media. *Advanced Hydroscience*, 10, 231–307.
- Cordonnier, M., 1984. La structure du bassin de la Haine et ses relations avec les circulations karstiques dinantiniennes. *Mémoires de l'Université Libre de Bruxelles*, 91 p.
- de Magnée, I., Delmer, A. & Cordonnier, M., 1986. La dissolution des anhydrites du Dinantien et ses conséquences. *Bulletin de la Société belge de Géologie*, 95, 213–220.
- De Putter, T., 1995. Etude sédimentologique de la Grande Brèche Viséenne ('V3a') du bassin de Namur-Dinant. *Mémoire pour servir à l'Explication des Cartes Géologiques et Minières de Belgique*, 40, 264 p.

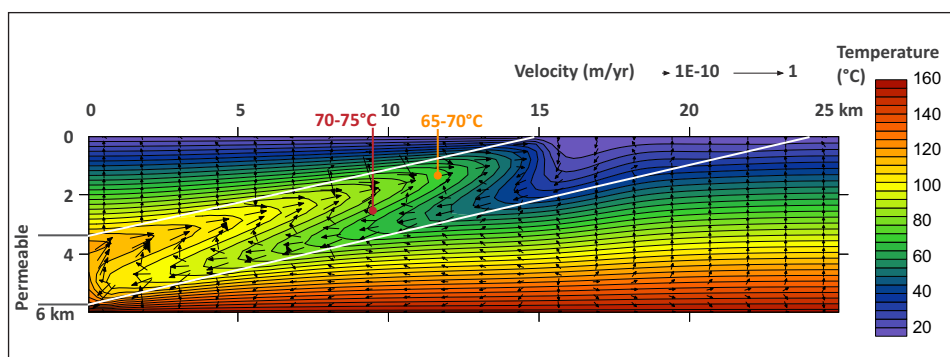


Figure 12. Simulated temperatures and velocity field in a simulated thick permeable stratum with a 10° dip, representing Dinantian limestone between Upper Carboniferous and Upper Devonian impervious strata. The alteration of the conductive temperature field by convection appears in this figure. The red and orange symbols respectively represent a projection of the Saint-Ghislain and Douvrain productive areas. The simulated temperatures are very similar to the fluid temperature measured at the two wells.

- De Putter, T., Groessens, E. & Herbosch, A., 1991. Le 'V3a' anhydritique du sondage de Saint-Ghislain (150E387, Province du Hainaut, Belgique): Description macroscopique et structures sédimentaires. Service Géologique de Belgique, Professional Paper 1991/6, 250, 22 p.
- De Putter, T., Rouchy, J.-M., Herbosch, A., Keppens, E., Pierre, C. & Groessens, E., 1994. Sedimentology and Palaeoenvironment of the Upper Visean anhydrite of the Franco-Belgian Carboniferous Basin (Saint-Ghislain borehole, Southern Belgium). *Sedimentary Geology*, 90, 77–93.
- Dejonghe, L., Delmer, A. & Groessens, E., 1976. Découverte d'anhydrite dans les formations anté-namuriennes du sondage de Saint-Ghislain (Note préliminaire). *Bulletin de l'Académie Royale de Belgique*, 80–83.
- Delmer, A., 1972. Origine du bassin crétacique de la Vallée de la Haine. Service Géologique de Belgique, Professional Paper 1972/5, 13 p.
- Delmer, A., 1977. Le bassin du Hainaut et le Sondage de Saint-Ghislain. Service Géologique de Belgique, Professional Paper 1977/6, 143, 11 p.
- Delmer, A., 1988. Le sondage de Saint-Ghislain (Pl. 150^E, n°387). Stratigraphie et tectonique en terrain houiller, sa liaison avec le sondage de Jeumont. *Annales de la Société Géologique de Belgique*, 111, 291–195.
- Delmer, A., 2004. Tectonique du Front Varisque en Hainaut et dans le Namurois. Mémoires du Service Géologique de Belgique, 50, 62 p.
- Delmer, A., Dusar, M. & Delambre, B., 2001. Upper Carboniferous lithostratigraphic units (Belgium). *Geologica Belgica*, 4, 95–103.
- Delmer, A., Leclercq, V., Marlrière, R. & Robaszynski, F., 1982. La géothermie en Hainaut et le sondage de Ghlin (Mons-Belgique). Annales de la Société Géologique du Nord, 101, 189–206.
- Delmer, A., Rorive, A. & Stenmans, V., 1996. Dix ans de géothermie en Hainaut. *Bulletin de la Société belge de Géologie*, 105, 77–85.
- Delmer, A. & Van Wichelen, P., 1980. Répertoire des puits naturels connus en terrain houiller du Hainaut. Service Géologique de Belgique, Professional Paper 1980/5, 172, 79 p.
- Dupuis, C. & Vandycke, S., 1989. Tectonique et karstification profonde : un modèle de subsidence pour le bassin de Mons. Annales de la Société Géologique de Belgique, 112, 479–
- Fiege, K., Bouckaert, J., Lambrecht, L., Scheere, J. & Van Tassel, R. 1967. Tranchée du canal Nimy-Antoing au Mont des Groseillers, Blaton. Viséen supérieur et Namurien inférieur. Service Géologique de Belgique, Professional Paper 1967/14, 203 p.
- Friedman, G. M., 1997. Dissolution-collapse breccias and paleokarst resulting from dissolution of evaporite rocks, especially sulfates. *Carbonates and Evaporites*, 12, 53–63.
- Groessens, E., Conil & Hennebert, M., 1979. Le Dinantien du Sondage de Saint-Ghislain. Stratigraphie et Paléontologie. Mémoire pour servir à l'Explication des Cartes Géologiques et Minières de Belgique, 22, 137 p.
- Hance, L. & Hennebert, M., 1980. On some Lower and Middle Visean Carbonate deposits of the Namur Basin, Belgium. *Mededelingen Rijks Geologische Dienst*, 32, 66–68.
- Hance, L., Hennebert, M. & Overlau, P., 1981. Révision stratigraphique et sédimentologique du Tournaisien supérieur (Ivorian) et du Viséen inférieur (Molinacién) de la vallée de l'Orneau, Belgique. Mémoires de l'Institut Géologique de l'Université de Louvain, 31, 183–207.
- Havron, C., Baele, J.-M. & Quinif, Y., 2007. Pétrographie d'une altérite résiduelle de type 'fantôme de roche'. *Karstologia*, 49, 25–32.
- Holser, W. T. & Kaplan, I. R., 1966. Isotope chemistry of sedimentary sulfate. *Chemical Geology*, 1, 93–135.
- Kaufmann, O., 2000. Les effondrements karstiques du Tournaisien : genèse, évolution, localisation, prévention. PhD Thesis Faculté Polytechnique de Mons.
- Krouse, H., 1980. R. Sulphur isotope in our environment. Handbook of Environmental Isotope Geochemistry. I : The Terrestrial Environment, 435–471.
- Lacquement, F., Mansy, J.-L., Hanot, F. & Meilliez, F., 1999. Retraitements et interprétation d'un profil sismique pétrolier méridien au travers du Massif paléozoïque ardennais (Nord de la France). *Comptes Rendus de l'Académie des Sciences de Paris*, 329, 471–477.
- Leclercq, V., 1980. Le Sondage de Douvrain. Service Géologique de Belgique, Professional Paper 1980/3, 170, 51 p.
- Legrand, R., 1978. La géothermie du Sondage de Saint-Ghislain. *Bulletin de la Société belge de Géologie*, 87, 168–169.
- Licour, L., 2009. L'aquifère géothermique du Hainaut (Belgique). Un karst profond à (re-) découvrir. *Karstologia Mémoires*, 17, 58–63.
- Licour, L., 2012. Relations entre la géologie profonde et le comportement hydrogéologique du réservoir géothermique du Hainaut (Belgique) - Caractérisation de l'aquifère dans la région de Saint-Ghislain. PhD Thesis Université de Mons, Faculté Polytechnique, 372 p.
- Licour, L., Quinif, Y. & Rorive, A., 2011. La géothermie profonde en Hainaut - Le réservoir du Dinantien. *Bulletin d'Information des Géologues du Bassin de Paris*, 48, 31–35.
- Licour, L., Rorive, A. & Mengeot, A., 2007. The aquifer of the Devonian Carboniferous Limestones of Hainaut (Belgium) : a karstified medium, a non-karstic behavior. *Geologica Belgica*, 10, 156–157.
- Mamet, B., Claeys, P., Herbosch, A., Préat, A. & Wolfowicz, P., 1986. La 'Grande Brèche' viséenne (V3a) des Bassins de Namur et de Dinant (Belgique) est probablement une brèche d'effondrement. *Bulletin de la Société belge de Géologie*, 95, 151–166.
- Mansy, J.-L., Everaerts, M. & De Vos, W., 1999. Structural analysis of the adjacent Acadian and Variscan fold belts in Belgium and Northern France from geophysical and geological evidence. *Tectonophysics*, 309, 99–106.
- Mansy, J.-L. & Lacquement, F., 2006. Contexte géologique régional : l'Ardenne Paléozoïque (Nord de la France et Sud de la Belgique). *Géologie de la France*, 1-2, 7–12.
- Mansy, J.-L. & Meilliez, F., 1993. Elements d'analyse structurale à partir d'exemples pris en Ardennes-Avesnois. *Annales de la Société Géologique du Nord*, 2 (2ème série), 45–60.
- Meilliez, F., 1989. Tectonique distensive et sédimentation à la base du Dévonien en bordure NE du Massif de Rocroi (Ardenne). *Annales de la Société Géologique du Nord*, 107, 281–295.
- Mook, W. G., 2000. Environmental isotopes in the hydrological cycle. Principles and Applications. *Technical Documents in Hydrology*, 39-1, 280 p.
- Overlau, P., 1963. Particularités sédimentaires du Calcaire de Basècles. *Bulletin de la Société belge de Géologie*, 72, 261–271.
- Overlau, P., 1966. La sédimentation viséenne dans l'Ouest du Hainaut belge. Thesis Université Catholique de Louvain, 130p.
- Pearson, F. J. & Rightmire, C. T., 1980. Sulfur and oxygen isotopes in aqueous sulfur compounds. *Handbook of Environmental Isotope Geochemistry*. I : The Terrestrial Environment, 227–258.
- Poty, E., Hance, L., Lees, A. & Hennebert, M., 2001. Dinantian lithostratigraphic units (Belgium). *Geologica Belgica*, 4, 69–94.
- Quinif, Y. & Licour, L., 2012. The karstic phenomenon of the Iguanodon sinkhole and the geomorphological situation of the Mons Basin during the Early Cretaceous. *Bernissart Dinosaures and the Early Cretaceous Terrestrial Systems*, 51–61.
- Quinif, Y., Meon, H. & Yans, J., 2006. Nature and dating of karstic filling in the Hainaut Province (Belgium). Karstic, geodynamic and paleogeographic implications. *Geodinamica Acta*, 19, 73–85.
- Quinif, Y., Vandycke, S. & Vergari, A., 1997. Chronologie et causalité entre tectonique et karstification. L'exemple des paléokarsts Crétacés du Hainaut (Belgique). *Bulletin de la Société Géologique de France*, 168, 463–472.
- Quinif, Y., Vergari, A., Doremus, P., Hennebert, M. & Charlet, J.-M., 1993. Phénomènes karstiques affectant le Calcaire Carbonifère du Hainaut. *Bulletin de la Société belge de Géologie*, 102, 379–394.
- Quinif, Y., 1989. Paleokarsts in Belgium. Paleokarsts. A systematic and regional review. 35–50.
- Rouchy, J.-M., Groessens, E. & Laumondais, A., 1984. Sédimentologie de la formation anhydritique viséenne du sondage de Saint-Ghislain (Hainaut, Belgique) - Implications paléogéographiques et structurales. *Bulletin de la Société belge de Géologie*, 93, 105–145.
- Rouchy, J.-M., Groessens, E. & Laumondais, A., 1993. Dislocation des formations évaporitiques par la tectonique et la dissolution : le modèle des évaporites dinantiennes du domaine varisque franco-belge. *Bulletin de la Société Géologique de France*, 164, 39–50.
- Rouchy, J.-M., Pierre, C., Groessens, E., Monty, C., Laumondais, A. & Moine, B., 1986. Les évaporites pré-permiennes du segment varisque franco-belge : Aspects paléogéographiques et structuraux. *Bulletin de la Société belge de Géologie*, 95, 139–149.
- Spagna, P., 2010. Les faciès wealdiens du Bassin de Mons (Belgique) : paléoenvironnements, géodynamique, et valorisation industrielle. PhD Thesis Université de Mons, 123 p.
- Stevens, C. & Marlrière, R., 1944. Révision de la carte du relief du socle paléozoïque du Bassin de Mons. *Annales de la Société Géologique de Belgique*, 67, 145–175.
- Vanbrabant, Y., Braun, J. & Jongmans, D., 2002. Models of passive margin inversion : implication of the Rhenohercynian fold-and-thrust belt, Belgium and Germany. *Earth and Planetary Science Letters*, 202, 15–29.
- Vandycke, S., 2007. Déformations cassantes du Nord-Ouest européen. Thèse Faculté Polytechnique de Mons, 462 p.
- Vergari, A. & Quinif, Y., 1997. Les paléokarsts du Hainaut (Belgique). *Geodinamica Acta*, 10, 4, 175–187.
- Ziegler, P. A., 1990. Geological atlas of Western and Central Europe. Shell Internationale Petroleum Maatschappij, 239 p.